

**NOVEL IMAGE PROCESSING APPLICATIONS OF A BIREFRINGENT
LENS IN THE INFRARED REGION**Pranati Mandal¹, Sandeep Kumar²¹Ptu Roll No.- 1168657 Master Of Technology, Electronics And Communication, Punjab College Of Engineering & Technology, Lalru²Assistant Professor, Electronics and Communication Engineering, PCET, Lalru.

ABSTRACT: The techniques for pre-specified modification of the imaging characteristics of an optical system received considerable attention since the early days of systematic investigation of optical imagery [1-2]. It was found that the pupil function of any optical system plays an important role in this regard. The desired modification of the imaging characteristics is usually implemented by using a mask on the pupil of the optical system. Extensive studies have been carried out in this direction and the use of amplitude masks and phase masks have been reported [3-7]. Usually each mask is dedicated to a specific purpose and on-line modification of such masks is not possible. At the same time, synthesis of the pupil function for yielding a specific imaging characteristic is indeed a formidable task and remains practically insolvable except for some limitingly terminal and simple cases.

It has been recognized that the polarization properties of light, if ingeniously used, offers additional flexibilities to the optical designers that are unachievable by scalar wave properties alone [8-16]. The advantage of these polarization-based optical systems is that their imaging properties can be continuously altered in situ. Polarization is used as a parametric variable to introduce a variation in the complex amplitude of the pupil. Obviously, two degrees of freedom due to two orthogonal states of variation are available to continually change the imaging properties of these systems by varying the relative contributions of the two orthogonal components. However, fabrication and accurate alignment of such masks are quite troublesome and a considerable loss of light due to absorption, scattering etc. takes place in the masking element. Thus, a system, easily realizable, equally effective as well as free from the previously stated problems, had long been a requirement. Optical systems fabricated with birefringent materials have this potential and this motivated many researchers to investigate the behaviour of a birefringent lens made of a uniaxial crystal [17-26]. A uniaxial birefringent lens sandwiched between two linear polarizers with its optic axis perpendicular to the lens axis behaves like an ordinary lens with a radially varying complex filter at its pupil plane [17-18]. Since the filter is generated because of the interference phenomenon, the problem associated with the alignment is removed. The imaging characteristics of the said system can be altered continuously just by changing the orientation of the any of the two polarizers. This makes the proposed system more versatile.

The imaging characteristics of the proposed system under diffraction-limited condition were studied [17-21]. The same system may be adapted either for enhanced resolution or for apodization just by rotating any polarizers included in the system. This system behaves as a double focus lens in general and by varying the birefringent lens parameters it is possible to change the separation between the two foci. The proposed system may be designed to obtain noticeably high depth-of-focus compared to an identical ordinary lens [19]. The imaging characteristics of the proposed system in presence of pre-specified on-axis and off-axis aberrations were studied [22-24]. It shows higher tolerance to the aberrations than an identical conventional lens. The effect of polychromatic visible light on the performance of the system was also investigated [25]. The study revealed that the focusing characteristics of the proposed system do not change appreciably under polychromatic illumination from that under strictly monochromatic illumination. The need for appropriate infrared imaging devices and components has been on the rise [27-34]. The applications of proposed system under monochromatic or polychromatic beam illumination in the infrared region have not been explored till date. We study the viability of the proposed system considering crystal quartz as the birefringent lens material in the infrared region. In this connection it may be mentioned that the coefficient of absorption for the crystal quartz is less than 0.030 cm^{-1} in the region approximately from 190 nm to 2900 nm [35]. The infrared band is often subdivided into smaller sections though the divisions are different for different applications [36]. We consider the range of wavelengths for which infrared photography (700 nm to 900 nm) and short-wave infrared (SWIR) defence applications (900 nm to 1700 nm) usually take place. The wavelength of around 1550 nm is used for modern fiber-optic communication [37]. Thus the proposed system may find applications in multiple domains, such as SWIR defence and surveillance purposes, infrared photography, medicine, archaeology, modern fiber-optic communication systems and many other infrared imaging devices. The axial irradiance distribution function and the intensity point spread function are considered as the image assessment parameters. The results show that all the above properties of the said system are retained even under infrared illumination having large bandwidth.

I. INTRODUCTION

The need for appropriate infrared imaging devices and components has been on the rise [1-8] because of the fact that infrared imaging is extensively used for military and civilian purposes. Military applications include target acquisition, surveillance, night vision, homing and tracking. Non-military uses include environmental monitoring, industrial facility inspections, wireless communication and modern fiber-optic communication, spectroscopy, weather forecasting, infrared photography and medical applications, to mention but a few. Infrared astronomy uses sensor-equipped telescopes for observation of objects obscured by interstellar dust. Infrared imaging cameras are utilized to detect heat loss in insulated systems, observe changing blood flow in the skin, and overheating of electrical apparatus [9,10].

Optical scientists have always been in search of techniques for better imagery in the infrared region that meet the requirements of the above-mentioned applications. It has been reported in the recent past that a uniaxial birefringent lens sandwiched between two linear polarizers has better depth-of-focus as well as higher tolerance to various aberrations than an equivalent isotropic glass lens [11-22]. The optic axis of the birefringent crystal is perpendicular to the lens axis. When illuminated with a monochromatic beam of light, such a system behaves like a conventional lens with a radially varying complex filter at its pupil plane [11-12]. Since the filter is generated because of the interference phenomenon, it is self-aligned, and no light loss occurs because of scattering and absorption in the masking element. The advantage of the proposed system is that the imaging characteristics of the said system can be continuously altered *in situ* just by rotating any of the two polarizers included in the system or during the fabrication of the lens. This makes the system more versatile and the same system may be adapted for different applications. The imaging characteristics of the proposed system under diffraction-limited condition with monochromatic input illumination were studied [11-15]. The same system may be adapted either for enhanced resolution or for apodization just by rotating any polarizer place before and after the birefringent lens. This system behaves as a double focus lens in general and by varying the birefringent lens parameters it is possible to change the separation between the two foci. The proposed system may be designed to obtain noticeably high depth-of-focus compared to an identical ordinary lens [13]. The imaging characteristics of the proposed system in presence of pre-specified on-axis and off-axis aberrations were studied [16-18]. It shows higher tolerance to the aberrations than an identical conventional lens. The effect of polychromatic visible light on the performance of the system was also investigated [19-22]. The study revealed that the imaging characteristics of the proposed system do not change appreciably under polychromatic illumination from that under strictly monochromatic illumination.

Here, we intend to study whether the proposed system retains some of the above-mentioned properties in the infrared region. Crystal quartz is selected as the birefringent lens material. It is to be noted that fused quartz has been used for several imaging systems as it can withstand enormous heating which conventional glass lenses are not able to. In this connection it may be mentioned that crystal quartz provides low birefringence which is also required for such a system [19]. The coefficient of absorption for the crystal quartz is less than 0.030 cm^{-1} in the region approximately from 190 nm to 2900 nm [22]. Thus, a single system may find applications in multiple domains, such as short-wave infrared (SWIR) defence and surveillance purposes (900-1700 nm), infrared photography (700-900 nm), medicine, archaeology, modern fiber-optic communication systems and many other infrared imaging devices. We study the imaging behaviour of the said system by means of the axial irradiance distribution function, the intensity point spread function (IPSF) and the optical transfer function (OTF). The results show that the same system maintains both apodization and enhanced resolution properties for two orthogonal positions of the second polarizer even when the spectral spread in the infrared region is very large. The depth-of-focus is also found to be very large for large spectral spread.

II. LITERATURE REVIEW

2.1 Introduction

In the previous chapter, the relative advantages of using a birefringent lens made of a uniaxial crystal over an equivalent glass lens and other polarization-based optical systems were discussed. The lens under consideration is sandwiched between two linear polarizers and the optic axis of the birefringent crystal is perpendicular to the system axis. When such a system is illuminated with a monochromatic beam of light with a state of polarization other than parallel or perpendicular to the optic axis of the lens, circular fringes are produced on the pupil plane of the system. Therefore, our proposed system behaves like a conventional lens with a radially varying complex mask generated on its pupil plane. The nature of this virtual mask can be modified to improve certain desirable qualities of the imaging system just by rotating any of the two polarizers included in the system or during the design and the fabrication of the birefringent lens. Such modification of the image quality is essential mainly to reduce aberrations, to increase the resolution and the depth-of-focus or for image processing applications. Hence, a detailed analysis of the pupil function for the proposed system is worth-mentioning. This chapter aims at presenting the working principle of the proposed system followed by a rigorous mathematical calculation and discussion on the pupil function for the said system.

2.2 Working Principle of the Proposed System

The construction of our proposed system has been shown in Fig. 2.1. The working principle of the said system is based on the fact that two orthogonally polarized spherical wavefronts of different radii of curvatures are produced if a beam of light with a state of polarization other than parallel or perpendicular to the optic axis of the lens ($\theta_1 \neq 0^\circ$ or 90°) illuminates the birefringent lens. In other words, the birefringent lens has two different foci, one for the ordinary rays and the other for the extraordinary rays and these two foci are longitudinally separated along the system axis. The two orthogonally polarized spherical wavefronts interfere after passing through the second polarizer ($\theta_2 \neq 0^\circ$ or 90°). This interference causes the formation of circular fringes like Newton's rings on the pupil plane of the said system. The orientation of the polarizers determines the relative contribution of the two orthogonal vibrations of light. Therefore, it may be concluded that the proposed system may be considered as an ordinary lens with a radially varying complex mask effectively formed on the aperture of the birefringent lens. The object is placed before the first polarizer and may be self-luminous or may be illuminated by unpolarized light.

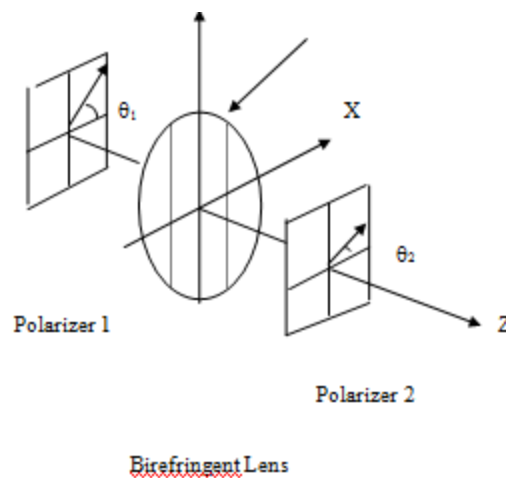


Fig. 2.1: A birefringent lens sandwiched between two linear polarizers

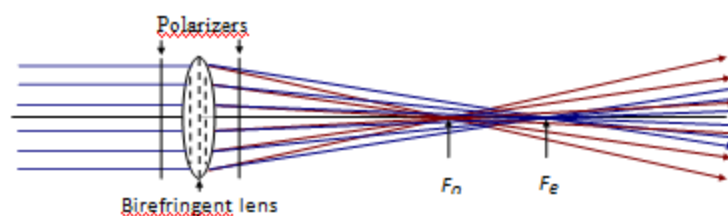


Fig. 2.2: Formation of two foci when a bundle of parallel rays passes

The above figure depicts how the ordinary rays are focused at F_o and extraordinary rays at F_e . Vector interference between the two orthogonally polarized beams having different radii of curvatures compels the resultant wave to converge at a different location.

2.3 Mathematical Formulation of the Pupil Function

The section is intended for thorough understanding of the nature of complex mask effectively formed at the pupil plane of the proposed system.

Let a monochromatic beam of light with plane wavefront having wavelength λ and amplitude unity be incident normally (positive Z-direction) on the first polarizer of the proposed system (Fig. 2.1). Since the crystal optic axis of the birefringent lens is along the Y-axis, the extraordinary wave vibrates along it while the ordinary one vibrates along the X-

axis. The ordinary and the extraordinary components of light will be $\cos \theta_1$ and $\sin \theta_1$ respectively. It is well-known that a lens basically transforms the phase of the input beam. The amount of phase introduced by a spherical lens of central thickness Δ and focal length f is given by

$$T_l(R) = \exp \left[i k \left(n \Delta - \frac{R^2}{2f} \right) \right] \quad (2.1)$$

where $k = \frac{2\pi}{\lambda}$ is the propagation constant; n is the refractive index of the lens material and R is the radius vector of the pupil plane. The focal length of a lens having a difference of curvature δC between its two surfaces, may be expressed as

$$\frac{1}{f} = (n - 1) \delta C \quad (2.2)$$

Let n_o and n_e be the ordinary and extraordinary refractive indices of the birefringent lens material respectively. Hence, the phase introduced in the ordinary beam by the birefringent lens is $\exp(i G_o)$ and that introduced in the extraordinary beam is $\exp(i G_e)$; where $G_o = k \left(n_o \Delta - \frac{R^2}{2f_o} \right)$ and $G_e = k \left(n_e \Delta - \frac{R^2}{2f_e} \right)$; f_o and f_e being the corresponding focal lengths given by the relations:

$$\frac{1}{f_{o,e}} = (n_{o,e} - 1) \delta C$$

Since the birefringent lens is followed by a second polarizer with its transmission axis making an angle θ_2 with the reference X-axis, the resultant phase transformation introduced by the system will be a vector addition of the components of the two orthogonally polarized spherical beams transmitted through it. In order to obtain an expression for it, we will employ the Jones' Calculus formalism of polarization phenomenon.

The Jones matrix $P(\theta)$ for a polarizer with the transmission axis at an arbitrary direction θ with respect to the X-axis is given by

$$P(\theta) = \begin{bmatrix} \cos^2 \theta & \cos \theta \sin \theta \\ \cos \theta \sin \theta & \sin^2 \theta \end{bmatrix}$$

and that for a birefringent lens with optic axis perpendicular to the principal axis may be written as

$$B_L(\nabla n) = \begin{bmatrix} \exp(i G_o) & 0 \\ 0 & \exp(i G_e) \end{bmatrix}$$

Hence, the Jones matrix for the said system may be expressed as

$$\begin{aligned} S &= P(\theta_2) B_L(\nabla n) P(\theta_1) \\ &= \begin{bmatrix} \cos^2 \theta_2 & \cos \theta_2 \sin \theta_2 \\ \cos \theta_2 \sin \theta_2 & \sin^2 \theta_2 \end{bmatrix} \begin{bmatrix} \exp(i G_o) & 0 \\ 0 & \exp(i G_e) \end{bmatrix} \begin{bmatrix} \cos^2 \theta_1 & \cos \theta_1 \sin \theta_1 \\ \cos \theta_1 \sin \theta_1 & \sin^2 \theta_1 \end{bmatrix} \\ &= \left[\exp(i G_o) \cos \theta_1 \cos \theta_2 + \exp(i G_e) \sin \theta_1 \sin \theta_2 \right] \begin{bmatrix} \cos \theta_1 \cos \theta_2 & \sin \theta_1 \cos \theta_2 \\ \cos \theta_1 \sin \theta_2 & \sin \theta_1 \sin \theta_2 \end{bmatrix} \end{aligned}$$

The matrix part determines the state of polarization of the output beam and also the overall amplitude. The first factor represents the radial amplitude variation [$A(R)$]. Thus,

$$A(R) = \cos \theta_1 \cos \theta_2 \exp(i G_o) + \sin \theta_1 \sin \theta_2 \exp(i G_e) \quad (2.3)$$

Eq. (2.3) clearly indicates that the amplitude transmittance of the system depends on the orientation of the transmission axes of the two polarizers and the nature of the lens, namely, lens material, shape, thickness etc. The dependence of the

complex amplitude function of the proposed system on θ_1 and θ_2 indicates the possibility of controlling it just by rotating either of the polarizers. On simplification,

$$A(R) = \cos \theta_1 \cos \theta_2 \cos G_o + \sin \theta_1 \sin \theta_2 \cos G_e + i(\cos \theta_1 \cos \theta_2 \sin G_o + \sin \theta_1 \sin \theta_2 \sin G_e) \quad (2.4)$$

The amplitude of $A(R)$ is expressed as

$$\begin{aligned} |A(R)| &= \left[(\cos \theta_1 \cos \theta_2 \cos G_o + \sin \theta_1 \sin \theta_2 \cos G_e)^2 + \right. \\ &\quad \left. (\cos \theta_1 \cos \theta_2 \sin G_o + \sin \theta_1 \sin \theta_2 \sin G_e)^2 \right]^{\frac{1}{2}} \\ &= \left[(\cos \theta_1 \cos \theta_2)^2 + (\sin \theta_1 \sin \theta_2)^2 + \frac{1}{2} \sin 2\theta_1 \sin 2\theta_2 \cos(G_o - G_e) \right]^{\frac{1}{2}} \quad (2.5) \end{aligned}$$

Now, $G_o - G_e = k \left[\left(n_o \Delta - \frac{R^2}{2f_o} \right) - \left(n_e \Delta - \frac{R^2}{2f_e} \right) \right] = k \delta n \Delta - \frac{k}{2} \delta n \delta C R^2 \quad (2.6)$

where $\delta n = n_o - n_e$ is the birefringence of the lens material and $\frac{1}{f_o} - \frac{1}{f_e} = (n_o - 1)\delta C - (n_e - 1)\delta C = \delta n \delta C$.

If we assume that the lens has zero thickness at the edge, the central thickness Δ is related to the lens aperture R_0 and surface curvatures by the relation

$$\Delta = \frac{R_0^2}{2} \delta C \quad (2.7)$$

Substituting this to Eq. (2.6),

$$G_o - G_e = k \delta n \Delta \left[1 - \left(\frac{R}{R_0} \right)^2 \right] = 2k \alpha (1 - r^2) \quad (2.8)$$

where $r = \frac{R}{R_0}$ is the normalized radial coordinate of the pupil plane ($0 \leq r \leq 1$) and

$\alpha = \frac{\delta n \Delta}{2}$ is a function of the birefringent lens parameters.

Substituting the expression for $G_o - G_e$ to Eq. (2.5), we have

$$|A(r)| = \left[(\cos \theta_1 \cos \theta_2)^2 + (\sin \theta_1 \sin \theta_2)^2 + \frac{1}{2} \sin 2\theta_1 \sin 2\theta_2 \cos \left\{ 2k \alpha (1 - r^2) \right\} \right]^{\frac{1}{2}} \quad (2.9)$$

The phase part of $A(R)$ is given by

$$\angle A(R) = \tan^{-1} \frac{\cos \theta_1 \cos \theta_2 \sin G_o + \sin \theta_1 \sin \theta_2 \sin G_e}{\cos \theta_1 \cos \theta_2 \cos G_o + \sin \theta_1 \sin \theta_2 \cos G_e} \quad (2.10)$$

Now, G_o and G_e may be rewritten as

$$\begin{aligned} G_o &= \frac{G_o + G_e}{2} + \frac{G_o - G_e}{2} \\ &= k \left(\frac{n_o + n_e}{2} \right) \Delta - \frac{k}{4} \left(\frac{1}{f_o} + \frac{1}{f_e} \right) R^2 + k \alpha (1 - r^2), \text{ using Eq. (2.8)} \\ &= k \bar{n} \Delta - \frac{k}{2} (\bar{n} - 1) \delta C R^2 + k \alpha (1 - r^2) \end{aligned}$$

$$= k \bar{n} \Delta - k (\bar{n} - 1) \Delta \left(\frac{R}{R_0} \right)^2 + k \alpha (1 - r^2), \text{ using Eq. (2.7)}$$

$$= k \left[\bar{n} \Delta - \{ (\bar{n} - 1) \Delta \} r^2 \right] + k \alpha (1 - r^2) = k (\gamma - \sigma r^2) + k \alpha (1 - r^2)$$

$$\text{or, } G_o = k (\gamma - \sigma r^2) + k \alpha (1 - r^2) \tag{2.11a}$$

Here, $\bar{n} = \frac{n_o + n_e}{2}$ is the mean refractive index of the lens material and $\gamma = \bar{n} \Delta$; $\sigma = (\bar{n} - 1) \Delta$; both solely depend on the birefringent lens parameters.

$$\text{Similarly, } G_e = \frac{G_o + G_e}{2} - \frac{G_o - G_e}{2} = k (\gamma - \sigma r^2) - k \alpha (1 - r^2) \tag{2.11b}$$

$$\text{Let } k (\gamma - \sigma r^2) = P \text{ and } k \alpha (1 - r^2) = Q$$

$$\text{Therefore, } G_o = P + Q \text{ and } G_e = P - Q.$$

Hence, using Eqs. (2.11a) and (2.11b) and substituting the values for P and Q , Eq. (2.10) reduces to

$$\begin{aligned} \angle A(r) &= \tan^{-1} \frac{\cos \theta_1 \cos \theta_2 \sin(P + Q) + \sin \theta_1 \sin \theta_2 \sin(P - Q)}{\cos \theta_1 \cos \theta_2 \cos(P + Q) + \sin \theta_1 \sin \theta_2 \cos(P - Q)} \\ &= \tan^{-1} \frac{\sin P \cos Q (\cos \theta_1 \cos \theta_2 + \sin \theta_1 \sin \theta_2) + \cos P \sin Q (\cos \theta_1 \cos \theta_2 - \sin \theta_1 \sin \theta_2)}{\cos P \cos Q (\cos \theta_1 \cos \theta_2 + \sin \theta_1 \sin \theta_2) - \sin P \sin Q (\cos \theta_1 \cos \theta_2 - \sin \theta_1 \sin \theta_2)} \\ &= \tan^{-1} \frac{\sin P \cos Q \cos(\theta_1 - \theta_2) + \cos P \sin Q \cos(\theta_1 + \theta_2)}{\cos P \cos Q \cos(\theta_1 - \theta_2) - \sin P \sin Q \cos(\theta_1 + \theta_2)} \\ &= \tan^{-1} \frac{\cos(\theta_1 - \theta_2) + \cot P \tan Q \cos(\theta_1 + \theta_2)}{\cot P \cos(\theta_1 - \theta_2) - \tan Q \cos(\theta_1 + \theta_2)} \\ &= \tan^{-1} \frac{\cos(\theta_1 - \theta_2) + \cot \{ k (\gamma - \sigma r^2) \} \tan \{ k \alpha (1 - r^2) \} \cos(\theta_1 + \theta_2)}{\cot \{ k (\gamma - \sigma r^2) \} \cos(\theta_1 - \theta_2) - \tan \{ k \alpha (1 - r^2) \} \cos(\theta_1 + \theta_2)} \end{aligned} \tag{2.12}$$

Thus, the effective pupil function of the proposed system may be expressed as

$$A(r) = |A(r)| e^{i \angle A(r)}$$

Hence, a birefringent lens sandwiched between two linear polarizers may be treated as a conventional lens with a complex spatial filter on the pupil plane. The nature of this virtual mask is a function of the birefringent lens parameters along with the orientations of the

transmission axes of the two polarizers. So, the mask can be modified according to the users' requirement by rotating any of the two polarizers in real time. However it is also possible to modify the lens during fabrication.

We have restricted our investigation to $\theta_1 = 45^\circ$ and $\theta_2 = \pm 45^\circ$ which will ensure maximum radial variation of the effective pupil function. Since the transmission axis of the first polarizer is inclined at 45° with respect to the positive X-direction, the ordinary and the extraordinary beams emerging from the birefringent lens will have equal amplitude. If the preferential direction of transmission of the second polarizer is either at 45° or at -45° with respect to the positive X-axis, then vector addition or subtraction between the two equal components of the two orthogonally polarized spherical beams of identical light amplitude results in circular fringe patterns of maximum contrast at the pupil plane; i.e. the in-phase and out-of-phase interference between the two components produces a high contrast amplitude variation at the pupil plane.

Case-1: Parallel-Polarizers Configuration

When $\theta_1 = \theta_2 = 45^\circ$, the transmission axes of both the polarizers are parallel. Henceforth this will be referred to as 'parallel-polarizers configuration' and will be denoted by '+' sign.

For parallel-polarizers configuration Eq. (2.9) reduces to

$$|A^+(r)| = \left[\left(\frac{1}{2}\right)^2 + \left(\frac{1}{2}\right)^2 + \frac{1}{2} \cos \{2k\alpha(1-r^2)\} \right]^{\frac{1}{2}} = \cos \{k\alpha(1-r^2)\}$$

and from Eq. (2.12), the corresponding phase part is obtained as

$$\angle A^+(r) = k(\gamma - \sigma r^2).$$

Therefore, for parallel-polarizers configuration, the pupil function of the proposed system becomes

$$A^+(r) = \cos \{k\alpha(1-r^2)\} \exp \left[i k (\gamma - \sigma r^2) \right] \quad (2.13)$$

Case-2: Crossed-Polarizers Configuration

When the transmission axes of the two polarizers are orthogonal, i.e., $\theta_1 = 45^\circ$, $\theta_2 = -45^\circ$, the case will be referred as ‘crossed-polarizers configuration’. This will be denoted by ‘-’ sign.

For this orientation of the transmission axes of the polarizers, Eq. (2.9) reduces to

$$|A^-(r)| = \left[\left(\frac{1}{2}\right)^2 + \left(-\frac{1}{2}\right)^2 + \frac{1}{2} \cdot 1 \cdot (-1) \cos \{2k\alpha(1-r^2)\} \right]^{\frac{1}{2}} = \sin \{k\alpha(1-r^2)\}$$

Using these values $\angle A^-(r)$ [see Eq. (2.12)] comes out to be

$$\angle A^-(r) = \frac{\pi}{2} + k(\gamma - \sigma r^2)$$

Hence, for crossed-polarizers configuration, the pupil function of the proposed system may be

written as

$$A^-(r) = \sin \{k\alpha(1-r^2)\} e^{i \left\{ k(\gamma - \sigma r^2) + \frac{\pi}{2} \right\}} = i \sin \{k\alpha(1-r^2)\} e^{i k(\gamma - \sigma r^2)} \quad (2.14)$$

When defocusing is introduced, the pupil function $A(r)$ modifies to $\Omega(r)$ according to the following relation:

$$\begin{aligned} \Omega(r) &= A(r) e^{i k W_{20} r^2} && \text{for } r \leq 1 \\ &= 0 && \text{otherwise} \end{aligned} \quad (2.15)$$

where W_{20} is the defocus coefficient. Combining Eqs. (2.13), (2.14) and (2.15), the pupil function of the proposed system for parallel- and crossed-polarizers configurations under defocused condition may be expressed as

$$\Omega_{\pm}^{\pm}(r) = \frac{\cos}{i \sin} \{k\alpha(1-r^2)\} e^{i k (\gamma + W_{20} r^2 - \sigma r^2)} \quad (2.16)$$

The term $e^{-i k \sigma r^2}$ in Eq. (2.16) represents a spherical phase factor, which indicates a shift of focus for the said system equivalent to that introduced by a converging lens having focal length $\frac{2f_o f_e}{f_o + f_e}$. This has no effect other than to shift

the image plane. The condition $W_{20} = \sigma$ determines the position of the Gaussian image plane for the proposed system and the new defect of focus $\bar{W}_{20} = W_{20} - \sigma$ may be measured from this plane. The constant phase factor $e^{i k \gamma}$ does not affect the image intensity pattern formed in anyway. $\frac{\cos}{\sin} \{k\alpha(1-r^2)\}$ gives the effective nature of the virtual mask formed on the pupil plane of the said system for parallel- and crossed-polarizers configurations. Hence, $\frac{\cos^2}{\sin^2} (D r^2)$ fringes (D being a constant that depends on the lens parameters) may be observed on the pupil of the

proposed system when viewed from the output side. In this connection it may be mentioned that α determines the number of interference rings formed on the lens aperture, while the orientation of the transmission axis of the second polarizer together with α determines the axial amplitude transmittance of the pupil. The parameter α may be termed as a design parameter as it is a function of the central thickness of the birefringent lens and the birefringence of the lens material. Obviously, each birefringent lens is associated with a specific value of α and any pre-specified value of α can be assigned during the fabrication of the lens.

III. Point Spread Function (IPSF) and Axial Irradiance Distribution Function Evaluation of Imaging Performance by Means of Intensity

3.1 Mathematical Formulation

When illuminated with a monochromatic beam of light, the IPSF of the proposed system under focused and defocused conditions with both parallel- and crossed-polarizers configurations may be given as

$$\text{IPSF}(W_{20}) = 4 \left| \int_0^1 \frac{\cos}{\sin} [k\alpha (1 - r^2)] \exp[ik(W_{20} - \sigma)r^2] J_0(\rho r) r dr \right|^2 \quad (3.1)$$

where $k=2\pi/\lambda$ is the propagation constant, W_{20} is the defocus coefficient, $\alpha = \delta n \frac{\Delta}{2}$ and $\sigma = (\bar{n} - 1)\Delta = \frac{2(\bar{n} - 1)}{\delta n} \alpha$ are two design parameters of the birefringent lens, n_o and n_e are the ordinary and extraordinary refractive indices respectively, $\delta n = n_e - n_o$ is the birefringence of the lens material, $\bar{n} = \frac{n_o + n_e}{2}$ is the mean refractive index of the lens material and Δ is the central thickness of the lens. It may be mentioned in this connection that the parameter α determines the number of interference rings formed on the aperture of the birefringent lens and σ indicates a shift of the focus for the said system with respect to the Gaussian image plane for an ordinary lens of similar dimensions. The IPSF (3.1) is symmetric about $W_{20} = \sigma$.

In order to evaluate the imaging behaviour of the proposed system under infrared broadband illumination, we employ the above IPSF expression under strictly monochromatic illumination. The wavelength dependent parameters are then identified and the modified expression is integrated over the specified wavelength range of the given polychromatic light with due consideration of the nature of variation of the wavelength dependent parameters with λ . Now, n_o and n_e vary with wavelength and so are δn and \bar{n} . It makes both α and σ wavelength dependent parameters. The nature of variation of these parameters with λ is,

however, a property of the crystal and is different for different crystals.

Identifying the λ -dependent terms, expression (3.1) may be rewritten as

$$\begin{aligned} \text{IPSF}_\lambda(W_{20}) &= 4 \left| \int_0^1 \frac{\cos}{\sin} [k_\lambda \alpha_\lambda (1 - r^2)] \exp[ik_\lambda (W_{20} - \sigma_\lambda)r^2] J_0(\rho r) r dr \right|^2 \quad (3.2) \\ &= 4 \left| \int_0^1 \frac{\cos}{\sin} [k_\lambda \alpha_\lambda (1 - r^2)] \cos[k_\lambda (W_{20} - \sigma_\lambda)r^2] J_0(\rho r) r dr \right. \\ &\quad \left. + i \int_0^1 \frac{\cos}{\sin} [k_\lambda \alpha_\lambda (1 - r^2)] \sin[k_\lambda (W_{20} - \sigma_\lambda)r^2] J_0(\rho r) r dr \right|^2 \\ &= 4 \left[\int_0^1 \frac{\cos}{\sin} [k_\lambda \alpha_\lambda (1 - r^2)] \cos[k_\lambda (W_{20} - \sigma_\lambda)r^2] J_0(\rho r) r dr \right]^2 \\ &\quad + 4 \left[\int_0^1 \frac{\cos}{\sin} [k_\lambda \alpha_\lambda (1 - r^2)] \sin[k_\lambda (W_{20} - \sigma_\lambda)r^2] J_0(\rho r) r dr \right]^2 \quad (3.3) \end{aligned}$$

For a polychromatic illumination having flat-top spectral profile with mean wavelength λ_0 and a spread of $2\delta\lambda$, the above expression becomes

$$\begin{aligned} \text{IPSF}_{\text{poly}}(W_{20}) = & \frac{4}{2\delta\lambda} \int_{\lambda_0-\delta\lambda}^{\lambda_0+\delta\lambda} \left[\int_0^1 \frac{\cos[k_\lambda \alpha_\lambda (1-r^2)]}{\sin[k_\lambda (W_{20} - \sigma_\lambda)r^2]} J_0(\rho r) r dr \right]^2 d\lambda \\ & + \frac{4}{2\delta\lambda} \int_{\lambda_0-\delta\lambda}^{\lambda_0+\delta\lambda} \left[\int_0^1 \frac{\cos[k_\lambda \alpha_\lambda (1-r^2)]}{\sin[k_\lambda (W_{20} + \sigma_\lambda)r^2]} J_0(\rho r) r dr \right]^2 d\lambda \end{aligned} \quad (3.4)$$

The above integral may be evaluated numerically by using 96-point Legendre-Gauss quadrature technique of integration [23] provided the nature of variation of α_λ and σ_λ with λ is known. The variation of both δn_λ and \bar{n}_λ with λ for quartz crystal in the infrared region can be obtained using standard table [24].

For a polychromatic illumination with flat-top spectral profile having mean wavelength λ_0 and a spread of $2\delta\lambda$, the axial irradiance distribution function for the proposed system (under diffraction-limited condition) with parallel and crossed-polarizers configurations is given by [13,19]

$$\begin{aligned} I_{\text{poly}}(W_{20}) = & \frac{1}{2\delta\lambda} \frac{1}{4} \int_{\lambda_0-\delta\lambda}^{\lambda_0+\delta\lambda} \left[\sin^2\{W_{20} - (\alpha_\lambda + \sigma_\lambda)\} + \sin^2\{W_{20} + (\alpha_\lambda - \sigma_\lambda)\} \right. \\ & \left. \pm 2 \sin\{W_{20} - (\alpha_\lambda + \sigma_\lambda)\} \sin\{W_{20} + (\alpha_\lambda - \sigma_\lambda)\} \cos\left(\frac{2\pi}{\lambda} \alpha_\lambda\right) \right] d\lambda \end{aligned} \quad (3.5)$$

The integral may again be calculated numerically by using 96-point Legendre-Gauss quadrature technique of integration [23].

3.2 Results and Discussions

It was reported [11-22] that for $\alpha \leq 0.375\lambda$, the birefringent lens offers enhanced resolution under parallel-polarizers configuration while with crossed-polarizers configuration the same system acts as an apodizer under monochromatic illumination. We consider $\alpha_{\lambda_0} = 0.25\lambda_0$ for further study. Figs. 3.1 and 3.2 show the variation of the IPSF for the said system at the Gaussian image plane under parallel- and crossed-polarizers configurations respectively at an operating wavelength (λ_0) of 1300 nm with spectral spreads ($2\delta\lambda$) of 0 nm, 200 nm, 400 nm and 800 nm. The IPSF for an ideal lens at the Gaussian image plane for monochromatic illumination has also been drawn for comparison.

It is revealed from the figures that a polychromatic input illumination does not affect considerably the inherent characteristics of enhanced resolution of such low-power birefringent lens (small α) under parallel-polarizers configuration even when the spectral spread is 800 nm. The same system retains the property of apodization under the crossed-polarizers configuration when the spread is as high as 400 nm.

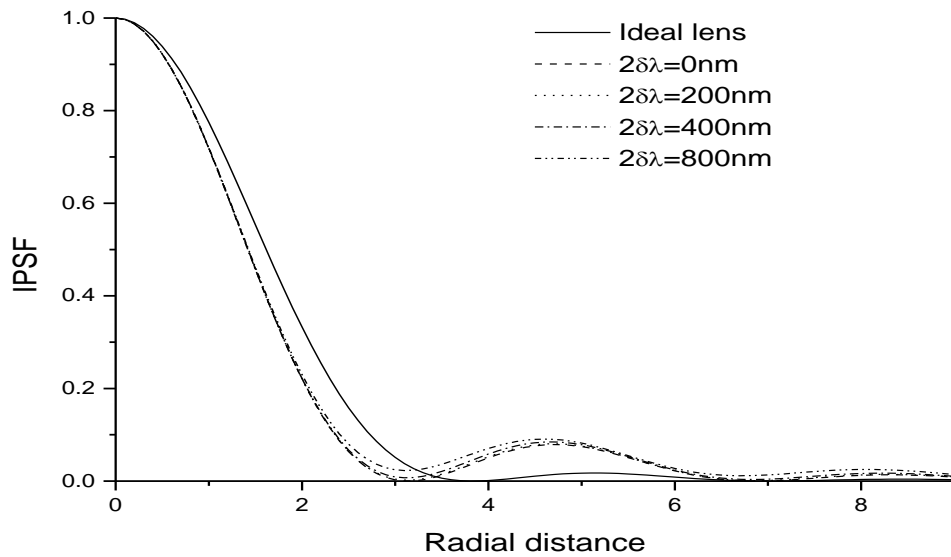


Fig. 3.1: The IPSP of a quartz crystal lens with $\alpha = 0.25\lambda_0$ at the Gaussian image plane under parallel-polarizers configuration. Ideal lens: solid line, birefringent lens: dotted/dashed line

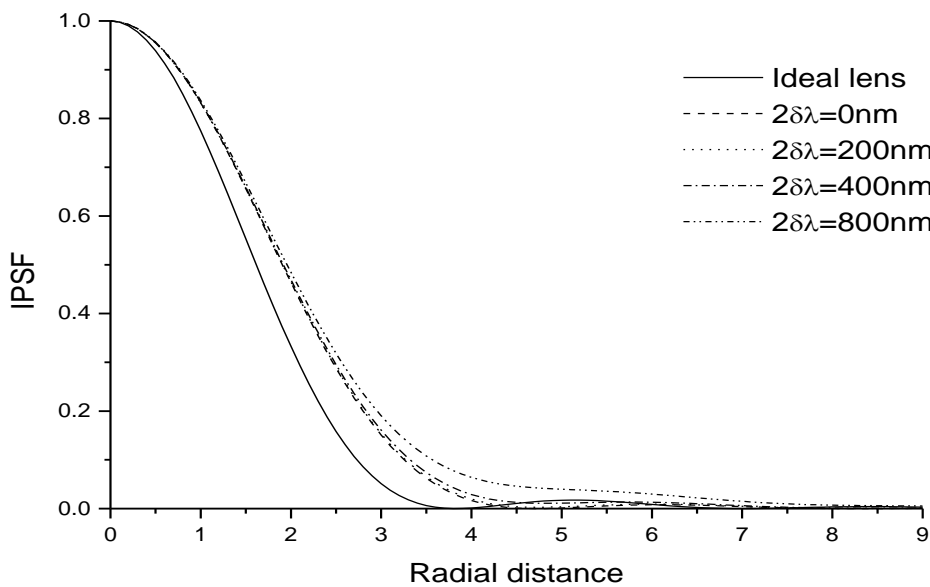


Fig. 3.2: Same as Fig. 3.1 except that the proposed system is under crossed-polarizers configuration

It was also reported that for $0.375\lambda < \alpha \leq 0.625\lambda$ with crossed-polarizers configuration, the system gives enhanced resolution for monochromatic input illumination. Fig. 3.3 shows the influence of polychromatic illumination on the IPSP curve for $\alpha_{\lambda_0} = 0.6044\lambda_0$ with crossed-polarizers configuration. In this connection it is to be mentioned that the said system offers the maximum depth-of-focus under diffraction-limited condition for $\alpha = 0.6044\lambda$ with crossed-polarizers configuration for monochromatic input illumination [13]. Now, an appreciable change in the IPSP curve takes place; in fact, the said system loses its characteristic of enhanced resolution at such a high value of α as depicted in Fig. 3.3. With further increase of α , the proposed system starts behaving as a double focus lens. Figs. 3.4 and

3.5 show the IPSF curve for $\alpha_{\lambda_0} = \lambda_0$ under crossed-polarizers configuration at a mean wavelength of 1300 nm and spectral spreads 100 nm and 250 nm respectively. The said system retains its bifocal nature when the spread is 100 nm. However, the birefringent lens loses this property at higher spectral spreads (Fig. 3.5) due to incoherent superposition of resultant monochromatic vectors and unequal phase retardation suffered by different wavelengths constituting the polychromatic beam along the system axis.

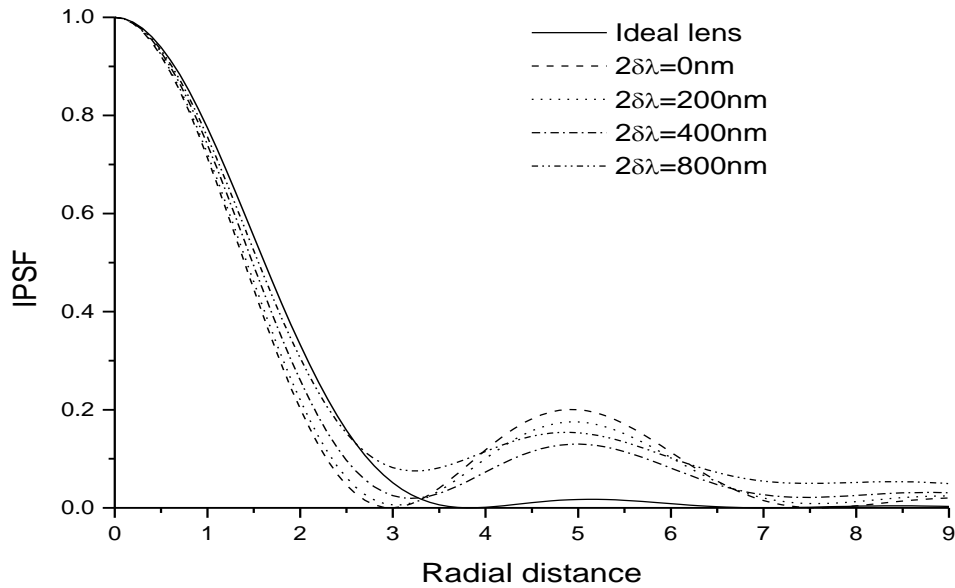


Fig. 3.3: Same as Fig. 3.1 except that the said system is under crossed-polarizers configuration and $\alpha = 0.6044 \lambda_0$

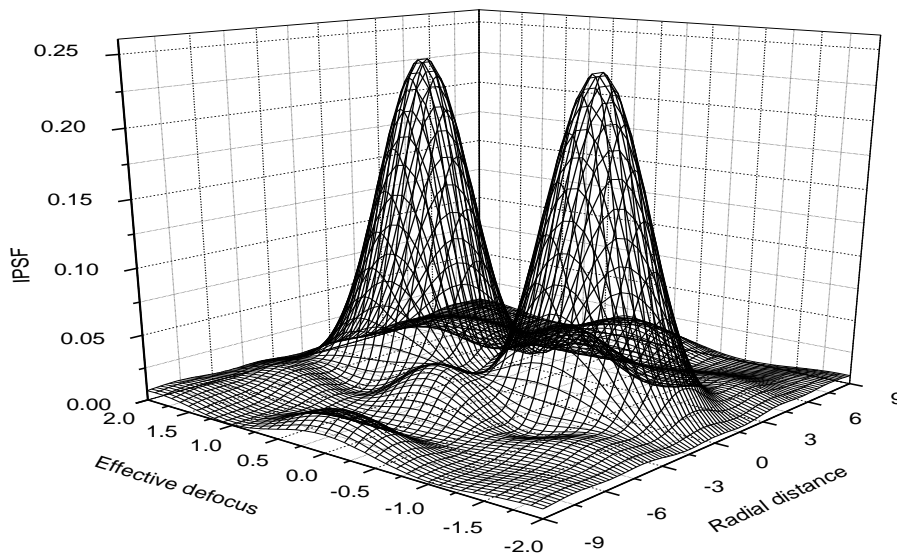


Fig. 3.4: Variation of IPSF with defocus for $\alpha = \lambda_0$ under crossed-polarizers configuration when illuminated with a polychromatic beam of mean wavelength 1300 nm and spectral spread 100 nm

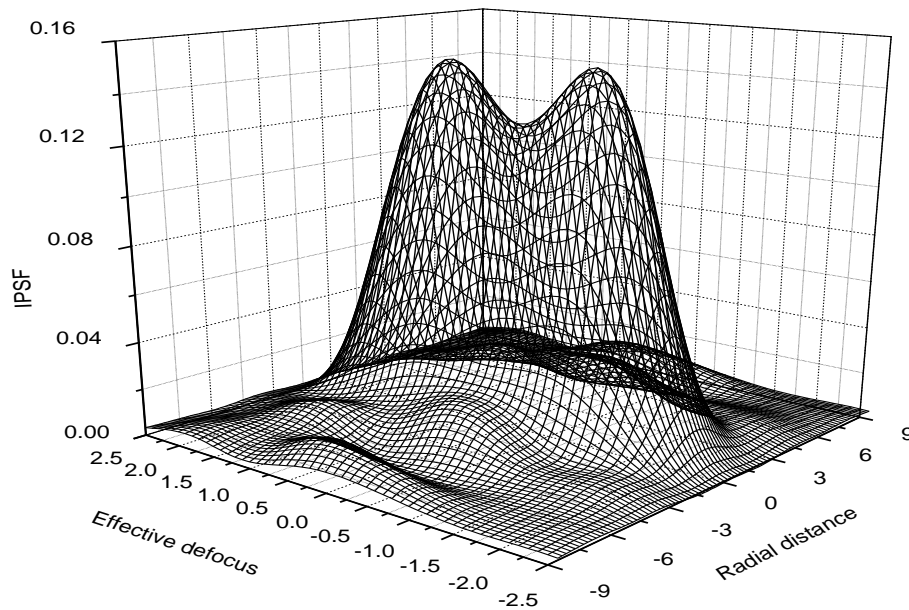


Fig. 3.5: Same as Fig. 3.4 except that the spectral spread is 250 nm

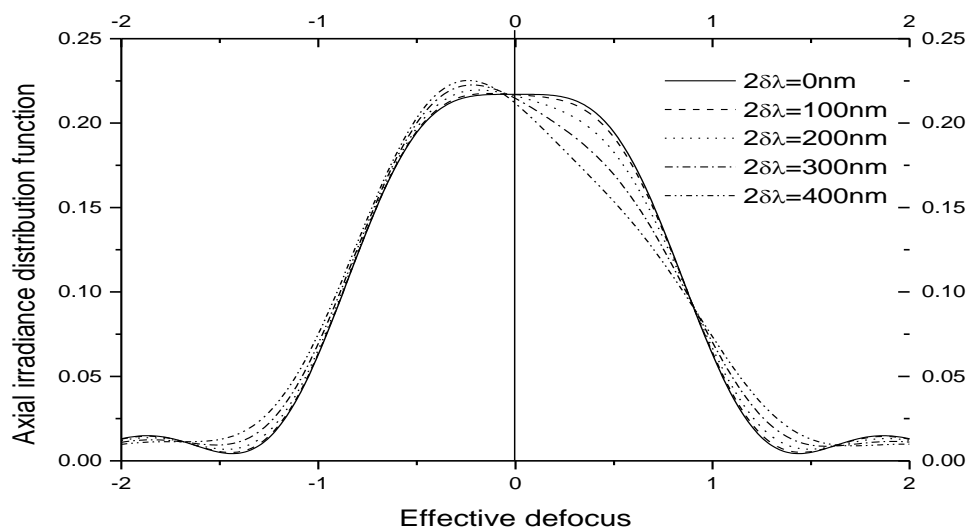


Fig. 3.6: The axial irradiance distribution for a crystal quartz lens with $\alpha = 0.3142\lambda_0$ under parallel-polarizers configuration

The proposed system offers the maximum depth of focus under diffraction-limited condition for $\alpha = 0.3142\lambda$ with parallel-polarizers configuration for monochromatic input illumination [13]. This motivated us to study the focusing characteristics of the system under infrared broadband illumination for this specific value of α . The axial irradiance distribution is computed for the proposed system under parallel-polarizers configuration at 1300 nm operating wavelength with spectral spreads of 0 nm, 100 nm, 200 nm, 300 nm and 400 nm (Fig. 3.6). It has been found that the allowable spectral bandwidth is approximately 100 nm at 1300 nm. The variation of the refractive indices as well as the

birefringence with wavelength in this region is less and almost linear for crystal quartz. Thus the asymmetry of the axial irradiance distribution becomes less even when the spectral spread is 100 nm.

The results for our proposed system shown so far are for the mean wavelength of 1300 nm. However, the system retains the same property throughout the wavelength range from 700 nm to 1700 nm.

IV. Evaluation of Imaging Performance by Means of Optical Transfer Function (OTF)

4.1 Mathematical Formulation

The normalized frequency response function for our proposed system with both parallel- and crossed-polarizers configurations under defocused condition for monochromatic input illumination [14,18] is given by

$$\begin{aligned}
 OTF_{-}^{+}(s, \alpha, \bar{W}_{20}) = & \frac{1}{N_{-}^{+}(\alpha)} \left[\int_{x=0}^a \int_{y=0}^b \cos [2k (\bar{W}_{20} - \alpha) s x] dx dy \right. \\
 & + \int_{x=0}^a \int_{y=0}^b \cos [2k (\bar{W}_{20} + \alpha) s x] dx dy \\
 & \pm \int_{x=0}^a \int_{y=0}^b \cos \left\{ 2k \alpha \left(x^2 + y^2 + \frac{s^2}{4} - 1 \right) + 2k \bar{W}_{20} s x \right\} dx dy \\
 & \left. \pm \int_{x=0}^a \int_{y=0}^b \cos \left\{ 2k \alpha \left(x^2 + y^2 + \frac{s^2}{4} - 1 \right) - 2k \bar{W}_{20} s x \right\} dx dy \right] \quad (4.1)
 \end{aligned}$$

where $k = 2\pi/\lambda$ is the propagation constant, $\bar{W}_{20} = W_{20} - \sigma$ is the effective defocus and W_{20} is the defocus coefficient. $\alpha = \delta n \frac{\Delta}{2}$ and $\sigma = (\bar{n} - 1)\Delta = \frac{2(\bar{n} - 1)}{\delta n} \alpha$ are two design parameters of the birefringent lens, n_o and n_e are the ordinary and extraordinary refractive indices respectively, $\delta n = n_e - n_o$ is the birefringence of the lens material, $\bar{n} = \frac{n_o + n_e}{2}$ is the mean refractive index of the lens material and Δ is the central thickness of the lens. s is the

normalized spatial frequency ($0 \leq s \leq 2$), $a = 1 - \frac{s}{2}$ and $b = \left[1 - \left(x + \frac{s}{2} \right)^2 \right]^{\frac{1}{2}}$. $N_{-}^{+}(\alpha) = \frac{\pi}{2} \left[1 \pm \text{sinc} \left(\frac{4\alpha}{\lambda} \right) \right]$ is

the

normalizing factor of the OTF for the proposed system and $\text{sinc}(\chi) = \frac{\sin(\pi\chi)}{\pi\chi}$. The parameter α determines the

number of interference rings formed on the aperture of the birefringent lens and σ indicates a shift of the focus for the said system with respect to the Gaussian image plane for an ordinary lens of similar dimensions. The OTF for the proposed system at the Gaussian image plane can be obtained by substituting $\bar{W}_{20} = W_{20} - \sigma = 0$ in Eq. (4.1).

In order to obtain a mathematical expression for the polychromatic OTF of our proposed system, the wavelength-dependent parameters of the above expression are identified. Then the expression is integrated over the specified wavelength range of the given polychromatic light considering the nature of the variation of the wavelength dependent parameters with λ . Thus, the polychromatic OTF of the said system for polychromatic illumination with flat-top spectral profile under both parallel-polarizers and crossed-polarizers configurations comes out as

$$\begin{aligned}
 & OTF_{-}^{+}(s_{\lambda}, \alpha_{\lambda}, \overline{W}_{20_{\lambda}}) \\
 &= \frac{1}{\int_{\lambda_1}^{\lambda_2} N_{-}^{+}(\alpha_{\lambda}) d\lambda} \left[\int_{\lambda_1}^{\lambda_2} \int_{x=0}^{a_{\lambda}} \int_{y=0}^{b_{\lambda}} \cos [2 k_{\lambda} \{ (W_{20} - \sigma_{\lambda}) - \alpha_{\lambda} \} s_{\lambda} x] dx dy d\lambda \right. \\
 &+ \int_{\lambda_1}^{\lambda_2} \int_{x=0}^{a_{\lambda}} \int_{y=0}^{b_{\lambda}} \cos [2 k_{\lambda} \{ (W_{20} - \sigma_{\lambda}) + \alpha_{\lambda} \} s_{\lambda} x] dx dy d\lambda \\
 &\pm \int_{\lambda_1}^{\lambda_2} \int_{x=0}^{a_{\lambda}} \int_{y=0}^{b_{\lambda}} \cos \left\{ 2 k_{\lambda} \alpha_{\lambda} \left(x^2 + y^2 + \frac{s_{\lambda}^2}{4} - 1 \right) + 2 k_{\lambda} (W_{20} - \sigma_{\lambda}) s_{\lambda} x \right\} dx dy d\lambda \\
 &\left. \pm \int_{\lambda_1}^{\lambda_2} \int_{x=0}^{a_{\lambda}} \int_{y=0}^{b_{\lambda}} \cos \left\{ 2 k_{\lambda} \alpha_{\lambda} \left(x^2 + y^2 + \frac{s_{\lambda}^2}{4} - 1 \right) - 2 k_{\lambda} (W_{20} - \sigma_{\lambda}) s_{\lambda} x \right\} dx dy d\lambda \right] \quad (4.2)
 \end{aligned}$$

where $a_{\lambda} = 1 - \frac{s_{\lambda}}{2}$ and $b_{\lambda} = \left[1 - \left(x + \frac{s_{\lambda}}{2} \right)^2 \right]^{\frac{1}{2}}$. The above expression is solved numerically using

the elegant and powerful 96-point Legendre-Gauss quadrature technique of integration [23]. The variation of n_o and n_e and hence, α_{λ} and σ_{λ} with λ in the IR region may be obtained from Ref. 24.

4.2 Results and Discussions

It was reported that for $\alpha \leq 0.375\lambda$, the birefringent lens offers enhanced resolution under parallel-polarizers configuration while with crossed-polarizers configuration the spread of the point spread function is more than normal indicating a lesser resolution under monochromatic illumination. We consider $\alpha_{\lambda_1} = 0.25\lambda_1$ for further investigation and concentrate ourselves in the wavelength range from 900 nm to 1700 nm which includes SWIR defence applications. The variation of the polychromatic OTF with spatial frequency at the Gaussian image plane for the said system under both parallel- and crossed-polarizers configurations is depicted in Figs. 4.1 and 4.2 respectively considering $\lambda_1 = 900$ nm with spectral spreads ($\Delta\lambda = \lambda_2 - \lambda_1$) equal to 0 nm, 600 nm and 800 nm. As evident from Fig. 4.1, the birefringent lens provides enhanced resolution for spectral spread up to 600 nm approximately in the infrared region. However, the system fails to maintain this property when the bandwidth is very large (say 800 nm). The same system retains its apodization property for crossed-polarizers configuration under broadband infrared illumination with a very large spectral spread (see Fig. 4.2). Thus, the proposed system may be adapted for either enhanced resolution or apodization just by rotating any of the polarizers even under the infrared illumination with large bandwidth.

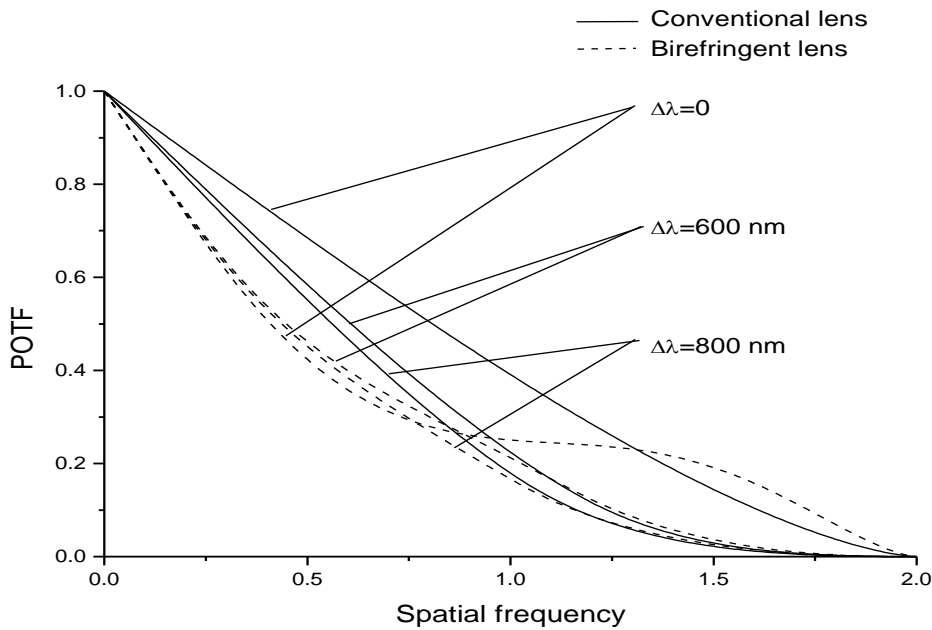


Fig. 4.1: Polychromatic OTF curves for a quartz lens with $\alpha_{\lambda_1} = 0.25\lambda_1$ at the Gaussian image plane under parallel-polarizers configuration when $\lambda_1 = 900\text{nm}$

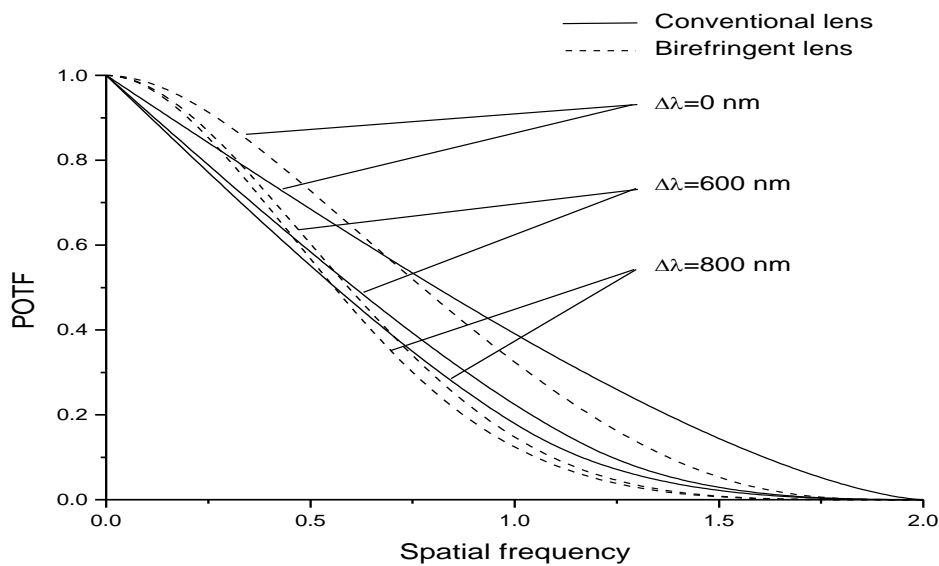


Fig. 4.2: Polychromatic OTF curves for a quartz lens with $\alpha_{\lambda_1} = 0.25\lambda_1$ at the Gaussian image plane under crossed-polarizers configuration when $\lambda_1 = 900\text{nm}$

V. CONCLUSIONS AND FUTURE SCOPE

We intend to study the imaging characteristics of an appropriate infrared imaging device which exhibits apodization, enhanced resolution and large depth-of-focus. The system should also show high tolerance to various on-axis and off-axis aberrations. These properties are essential for infrared imaging systems to be used for different military and non-military applications.

We consider an imaging system consisting of a uniaxial birefringent lens sandwiched between two linear polarizers. The optic axis of the birefringent crystal is perpendicular to the lens axis. Quartz crystal is chosen as the

birefringent lens material. When illuminated with a monochromatic beam of light, such a system behaves like a conventional lens with a radially varying complex filter at its pupil plane. Since the filter is generated because of the interference phenomenon, it is self-aligned, and no light loss occurs because of scattering and absorption in the masking element. The advantage of the proposed system is that the imaging characteristics of the said system can be continuously altered *in situ* just by rotating any of the two polarizers included in the system or during the fabrication of the lens. This makes the system more versatile and the same system may be adapted for different applications. The imaging characteristics of the said system are studied by means of the intensity point spread function and optical transfer function under both monochromatic and polychromatic input illumination. The study reveals that the system maintains both apodization and enhanced resolution properties for two orthogonal positions of the second polarizer under both monochromatic and polychromatic illumination. The focusing characteristics are studied in terms of axial irradiance distribution function. The results show that the proposed system also exhibits noticeably large-depth-focus for both monochromatic and polychromatic illumination.

REFERENCES

- [1]. Muyo . G, Singh. A , Andersson . M , Huckridge . D , Wood . A and Harvey A , “Infrared imaging with a wavefront-coded singlet lens,” *Opt. Exp.* 17, 21118-21123 (2009).
- [2]. Muyo . G and Harvey A . R , “Wavefront coding for athermalization of infrared imaging systems”, *Proc. SPIE* 5612, p. 227-235 (2004).
- [3]. Muyo . G , Harvey A. R , and Singh . A , “High-performance thermal imaging with a singlet and pupil plane encoding”, *Proc. SPIE* 5987, 162-169 (2005).
- [4]. Muyo . G , Singh . A , Andersson . M , Huckridge . D , and Harvey . A , “Optimized thermal imaging with a singlet and pupil plane encoding: experimental realization”, *Proc. SPIE* 6395, U211-U219 (2006).
- [5]. Benford D . J , Gaidis . M. C , and Kooi J . W , “Optical properties of Zitex in the infrared to submillimeter”, *Appl. Opt.* 42, 5118-5122 (2003).
- [6]. Lompadó . A , Sornsin . E. A and Chipman R. A , “HN22 sheet polarizer, an inexpensive infrared retarder”, *Appl. Opt.* 36, 5396-5402 (1997).
- [7]. Oliva . E , Gennari . S , Vanzi . L , Caruso . A and Ciofini . M , “Optical materials for near infrared Wollaston prisms”, *Astron. Astrophys. Suppl. Ser.* 123, 179-182 (1997).
- [8]. Hejazi . S , Spangler R. A , "A multi-wavelength thermal imaging system", *Engineering in Medicine and Biology Society, 1989. Images of the Twenty-First Century, Proc. of the Annual International Conference of the IEEE Engineering 4*, 1153-1154 (1989).
- [9]. <http://en.wikipedia.org/wiki/Infrared>
- [10]. Senior J. M , *Optical Fiber Communications: Principles and Practice*, pp. 91, Prentice-Hall of India, 2nd Ed., New Delhi (2003).
- [11]. Sanyal . S , Bandyopadhyay . P and A. Ghosh . A , “Vector wave imagery using a birefringent lens”, *Opt. Eng.* 37, 592-599(1998).
- [12]. Sanyal . S and Ghosh . A , “Imaging characteristics of birefringent lenses under focused and defocused condition”, *Optik* 110, 513-520 (1999).
- [13]. Sanyal . S and Ghosh . A , “High focal depth with a quasi-bifocus birefringent lens”, *Appl. Opt.* 39, 2321-2325 (2000).
- [14]. Sanyal . S and A . Ghosh . A , “Frequency response characteristics of a birefringent lens”, *Opt. Eng.* 41, 592-597 (2002).
- [15]. Sanyal . S and Ghosh . A , “Image assessment of a birefringent lens based on the factor of encircled energy”, *Opt. Eng.* 42, 1058-1064 (2003).
- [16]. Sanyal . S and Ghosh . A , “High tolerance to spherical aberrations and defects of focus using a birefringent lens”, *Appl. Opt.* 41, 4611-4619 (2002).
- [17]. Sanyal . S , Kawata . Y , Mandal . S and Ghosh . A , “High tolerance to off-axis aberrations with a birefringent lens”, *Opt. Eng.* 43, 1381-1386 (2004).
- [18]. Sanyal . S , Kawata . Y , Ghosh . A and Mandal . S , “Frequency response characteristics of a birefringent lens with off-axis aberrations”, *Appl. Opt.* 43, 3838-3847 (2004).
- [19]. Mandal . S , Sanyal . S and Ghosh . A , “Imaging characteristics of a birefringent lens under broadband illumination”, *Optik* 118, 335-339 (2007).
- [20]. Mandal . S and Ghosh . A , “Polychromatic intensity point spread function of a birefringent lens,” *Optik* 123, 1623-1626 (2012).
- [21]. Mandal . S , “Evaluation of polychromatic image quality of a birefringent lens by means of optical transfer function,” *Optik* 125, 121–125 (2014).

- [22]. Abramowitz . M and Stegun .IA , *Handbook of Mathematical Functions*, Dover Publications, INC., NY (1972).
- [23]. Luneburg,R. K. “Mathematical Theory of Optics, Brown University Press, Providence, R.I., p-391 (1944).
- [24]. Osterberg H. and Wilkins Jr., J. E. “The resolving power of a coated objective”, *J. Opt. Soc. Am.* 39, 553-557 (1949).
- [25]. Jacquinot ,P. and Roizen-Dossier ,B., “Apodization”, *Progress in Optics III*, ed. E. Wolf, p- 29-186, North-Holland, Amsterdam, (1964).
- [26]. Thompson,B. J. “Diffraction by semitransparent and phase annuli”, *J. Opt. Soc. Am.* 55, 145-149 (1965).
- [27]. Asakura ,T. and Mishina,H. “Diffraction by circular apertures with a ring shaped π -phase change”, *Japan. J. Appl. Phys.* 9, 195-202 (1970).
- [28]. Lit,J. W. Y. “Effects of a half wave filter in a portion of an aperture of a perfect lens”, *J. Opt. Soc. Am.* 61, 297-302 (1971).
- [29]. Chakraborty ,A. K. and Mukherjee,H. “Modification of PSF by polarisation mask”, *J. Opt. (India)* 5, 71-74 (1976).
- [30]. Chakraborty , A. K. , Mondol, B. , Adhikari and Roychoudhury , R. “The optical transfer function of a perfect lens with polarization masks ”, *J. Opt. (Paris)* 9, 251 -254 (1978).
- [31]. Ghosh A., Basu J., Goswami P. P. and Chakraborty,A. K., “Frequency response characteristics of a perfect lens partially masked by a retarder”, *J. Mod. Opt.* 34, 281-289 (1987).
- [32]. Ghosh A. , Murata K. and Chakraborty , A. K. , “Frequency response characteristics of a perfect lens masked by polarizing devices”, *J. Opt. Soc. Am. A.* 5, 277-284(1988).
- [33]. Bhattacharya ,K., Ghosh ,A. and Chakraborty ,A. K., “Realization of phase and amplitude steps on lens aperture using polarization masks”, *J. Opt.* 20, 128-131 (1991).
- [34]. Bhattacharya, K, Ghosh, A. and Chakraborty, A. K., “Vector wave imagery with a lens masked by polarizers”, *J. Mod. Opt.* 40, 379-390 (1993).
- [35]. Bhattacharya,K., Chakraborty, A. K. and Ghosh ,A., “Simulation of effects of phase and amplitude coatings on the lens aperture with polarization masks”, *J. Opt. Soc. Am. A.* 11, 586-592 (1994).
- [36]. Datta, S. N., Ghosh ,A. and Chakraborty ,A. K., “Imaging characteristics of a lens zonally masked by polarizers and retarder”, *Optik* 100, 1-7 (1995).
- [37]. Sanyal, S. , Ph D thesis , “Vector wave imagery using a birefringent lens “, 2001.
- [38]. Muyo ,G., Singh A., Andersson M., Huckridge D., Wood ,A. and Harvey A., “Infrared imaging with a wavefront-coded singlet lens,” *Opt. Exp.* 17, 21118-21123 (2009).
- [39]. Muyo ,G. and Harvey ,A. R., “Wavefront coding for athermalization of infrared imaging systems”, *Proc. SPIE* 5612, p. 227-235 (2004).
- [40]. Muyo ,G., Harvey ,A. R., and Singh A., “High-performance thermal imaging with a singlet and -pupil plane encoding”, *Proc. SPIE* 5987, 162-169 (2005).
- [41]. Muyo ,G., Singh,, Andersson ,M., Huckridge D., and Harvey ,A., “Optimized thermal imaging with a singlet and pupil plane encoding: experimental realization”, *Proc. SPIE* 6395, U211-U219 (2006).
- [42]. Benford ,D. J., Gaidis, M. C., and . Kooi ,J. W, “Optical properties of Zitex in the infrared to submillimeter”, *Appl. Opt.* 42, 5118-5122 (2003).
- [43]. Lompadó ,A., Somsin ,E. A., and Chipman ,R. A., “HN22 sheet polarizer, an inexpensive infrared retarder”, *Appl. Opt.* 36, 5396-5402 (1997).
- [44]. Oliva ,E., Gennari ,S., Vanzi ,L., Caruso, A. and Ciofini M., “Optical materials for near infrared Wollaston prisms”, *Astron. Astrophys. Suppl. Ser.* 123, 179-182 (1997).
- [45]. Hejazi ,S., Spangler ,R. A., "A multi-wavelength thermal imaging system", *Engineering in Medicine and Biology Society*, 1989. Images of the Twenty-First Century, *Proc. of the Annual International Conference of the IEEE Engineering* 4, 1153-1154 (1989).
- [46]. R. Straubel, Peter Zeeman *Verhandelingen, Nijhoff, The Hague* (1935).
- [47]. Mandal . S and Ghosh . A , “The effect of broadband illumination on the imaging characteristics of a birefringent lens suffering from primary spherical aberration”, *J. Opt. (India)* 40, 198-205 (2011).
- [48]. Ghosh,,A.,Chakraborty A. K, and Murata,K, “Imaging characteristics of a perfect lens partially masked by a linear polarizer”, *Optik* 76, 153-156 (1987).